

# Tunneling mediated by conical waves in a 1D lattice

Andrea Di Falco,<sup>1</sup> Claudio Conti,<sup>2,3</sup> Stefano Trillo<sup>3,4\*</sup>

<sup>1</sup> *School of Physics and Astronomy, University of St. Andrews, North Haugh, St. Andrews, KY16 9SS, UK*

<sup>2</sup> *Centro Studi e Ricerche “Enrico Fermi”, Via Panisperna 89/A, 00184 Rome, Italy*

<sup>3</sup> *Research center SOFT INFM-CNR Università di Roma “Sapienza”, P. A. Moro 2, 00185, Roma, Italy*

<sup>4</sup> *Dipartimento di Ingegneria, Università di Ferrara, Via Saragat 1, 44100 Ferrara, Italy*

(Dated: October 26, 2018)

The nonlinear propagation of 3D wave-packets in a 1D Bragg-induced band-gap system, shows that transverse effects (free space diffraction) affect the interplay of periodicity and nonlinearity, leading to the spontaneous formation of fast and slow conical localized waves. Such excitation corresponds to enhanced nonlinear transmission (tunneling) in the gap, with peculiar features which differ on the two edges of the band-gap, as dictated by the full dispersion relationship of the localized waves.

Localized wave-packets (LW) characterized by a conical envelope, and in particular X waves, have been invoked as a new paradigm that allows to explain several *nonlinear* optical wave phenomena observed in dispersive media, such as fsec trapping via frequency doubling and filamentation in Kerr-like media [1, 2, 3, 4], as well as spatio-temporal localization in lattices [5]. Unlike solitons, these LW exist also in the *linear* limit where they are expressed as superpositions of Bessel beams, well known in different context of physics [6, 7, 8]. The nonlinearity “dresses” these solutions, playing a key role (often strongly dynamical [2, 3]) in their formation and morphing process.

It has been suggested that LW can also exist as envelope modulations of linear Bloch modes in periodic media such as 1D lattices (with free diffraction in the transverse direction) [9], or 3D generalizations, namely photonic crystals [10, 11]. In this case they play a major role around the forbidden band-gaps where, however, strong reflection is expected to severely hamper their formation in the linear regime. While in principle the nonlinearity can be envisaged to favour the energy coupling and thus the excitation of LW, the dynamics of this process is completely unexplored so far. Furthermore, one can argue that conical LW can compete with gap soliton bullets (GB) [12, 13, 14], which are the multi-dimensional analog (usually under more restrictive conditions) of well-known gap solitons of 1D settings [15], observed, e.g., as slow light pulses in fiber Bragg gratings [16, 17], spatial envelopes in array of coupled waveguides [18], or atom clouds in a ultracold Bose condensed gas with standing wave optical lattice [19].

In this Letter we investigate the dynamic role of LW owing to additional free transverse dynamics (diffraction) included in a system with stop-band (whose 1D longitudinal dynamics and gap solitons are well known [15, 16, 17, 18, 19]). Employing excitations easily implementable in experiments (unidirectional and bell-shaped beams), we show numerically that, in lattices of finite length, highly transmissive nonlinear behavior in the stop-band is mediated by the excitation of conical LW. The features of this process can be understood on the ba-

sis of the linear multi-dimensional dispersion relationship of fast and slow LW, which entails a different dynamics on the two edges of the stopband. While on the lower edge, LW have a primary role to determine the enhanced nonlinear transmission, on the upper edge LW compete with GB, and their excitation stems from components tunneling through the gap in transverse wave-number. Thus our results suggest that gap solitons are not the sole entities that rule multi-dimensional nonlinear transmission through a stop-band.

We start from the following continuous model that rules (in dimensionless units) the propagation around a single Bragg resonance of a period 1D system [9, 13, 15]

$$\left(i\partial_t + i\partial_z + \frac{1}{2}\nabla_{\perp}^2\right)u_+ + u_- + \chi\left(|u_+|^2 + 2|u_-|^2\right)u_+ = 0, \quad (1)$$

$$\left(i\partial_t - i\partial_z + \frac{1}{2}\nabla_{\perp}^2\right)u_- + u_+ + \chi\left(|u_-|^2 + 2|u_+|^2\right)u_- = 0,$$

where  $t$  and  $z$  are normalized time and distance (along the 1D lattice), and  $\nabla_{\perp}^2 = \partial_x^2 + \partial_y^2$  is the transverse Laplacian. Though we expect a similar scenario with radially symmetric beams in two transverse dimensions, we discuss the computationally less demanding case of one transverse dimension ( $\nabla_{\perp}^2 = \partial_y^2$ ). In this case Eqs. (1) hold for Bragg optical gratings in a slab waveguide, or for Bose-Einstein atom condensates with free kinetic spreading (no trap in  $y$ ) transversally to a standing wave potential  $\sin^2(k_g z/2)$ . In the former case  $t, z, y$  are measured in units of  $T_0 = (V_g\Gamma)^{-1}$ ,  $Z_0 = \Gamma^{-1}$ ,  $Y_0 = (2k_0 n_{2I}\Gamma)^{-1/2}$ , respectively, whereas  $u_{\pm} = \sqrt{k_0 |n_{2I}|/2\eta} E_{\pm}$ ,  $E_{\pm}$  are counterpropagating envelopes at Bragg frequency,  $k_0$  and  $\eta$  are the relative vacuum wavenumber and impedance of the host medium,  $\Gamma$  is the Bragg coupling coefficient, and  $n_{2I}$  the Kerr nonlinear index. In the latter case, Eqs. (1) derive from the mean-field Gross-Pitaevskii (GP) equation [9] with  $T_0 = \hbar/\Gamma$ ,  $Z_0^2 = \hbar^2 k_g/(2m\Gamma)$ ,  $Y_0^2 = \hbar^2/m\Gamma$ ,  $m$  being the atomic mass whereas  $4\Gamma$  is the peak energy of the periodic potential.  $\psi_{\pm} = a^{-1/2}u_{\pm}$  are mutually Bragg scattered components of the atomic wave-function, with  $a = (4\pi\hbar^2/m)a_s$ ,  $a_s$  being the scattering length. In

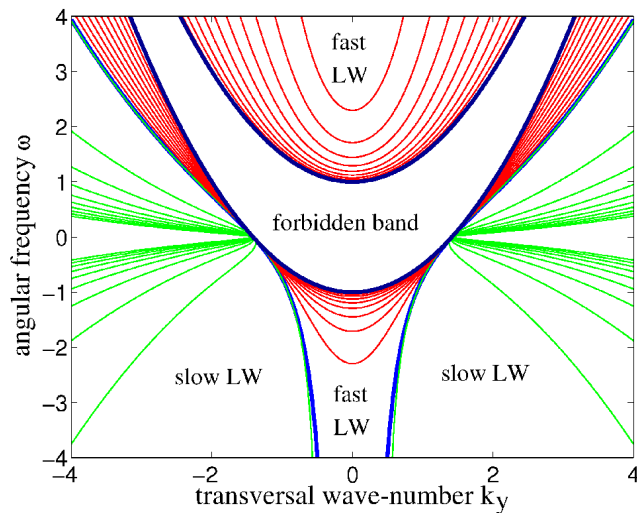


FIG. 1: (Color online) Spatio-temporal dispersion curves  $k_z = \omega/v$  of LW in the frequency plane  $k_y, \omega$ . Outside the forbidden band (region between the two parabolas), the LW light-line ( $v = 1$ , blue curve) divides the regions of subluminal LW ( $v < 1$ , green thin curves) and superluminal LW ( $v > 1$ , thick red curves).

the following we restrict the discussion to the focusing (or attractive) case i.e.  $\chi = \text{sign}(n_{2I}) = -\text{sign}(a_s) = 1$ , though similar phenomena can occur also in the defocusing (repulsive) case.

The reconstruction of the overall field or wave function (apart from inessential common phase shifts)  $u = u_+ \exp(ik_g z/2) + u_- \exp(-ik_g z/2)$ , shows the nature of the envelopes  $u_{\pm}$  as modulations of Bloch modes.

*Dispersion and localized wave spectra.* — The linear dispersion [ $u_{\pm} \sim \exp(ik_z z + ik_y y - i\omega t)$ ] relationship associated with Eqs. (1) reads as  $k_z^2 = (\omega - k_y^2/2)^2 - 1$ , which entails a lower (LB) and upper branch (UB) separated by a forbidden band in  $\omega$  (or energy). This gap of edges  $\omega_{\pm} = k_y^2/2 \pm 1$ , has constant width and central frequency shifting upward (parabolically) with  $k_y$  (tilted waves with  $k_y \neq 0$  see an effectively shorter period). While the UB  $\omega_+(k_y, k_z)$  has always positive curvature, it is near the saddle-shaped (i.e.,  $d^2\omega/dk_z^2 d^2\omega/dk_y^2 < 0$ ) LB  $\omega_-(k_y, k_z)$  that X-shaped LW has been predicted on the basis of a multiscale perturbative approach [9]. However, at the linear level ( $\chi = 0$ ), more general existence conditions for non-dispersive LW require simply a linear dependence  $k_z = \omega/v$ , where the arbitrary parameter  $v = dk_z/d\omega^{-1}$  stands for the group velocity of the LW travelling undistorted [2]. Upon substitution in the dispersion relationship we obtain the dispersion curves of LW, namely  $(\frac{\omega}{v})^2 = (\omega - k_y^2/2)^2$ , shown in the plane  $(k_y, \omega)$  (see Fig. 1) for various values of  $v$  below and above the luminal curve  $v = 1$ , denoted henceforth as the *LW light-line*. The dispersion curves do not involve evanescent waves and lie outside the gap (white region

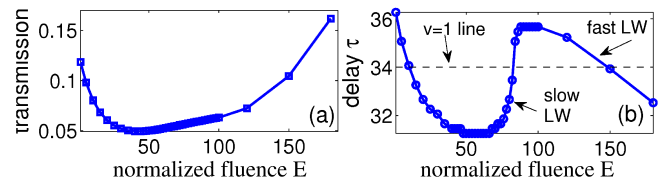


FIG. 2: (Color online) Excitation close to LB ( $\bar{\omega} = -0.99$ ). (a) Transmission Vs input fluence  $E$ ; (b) Output pulse delay  $\tau$  Vs  $E$ . The delay is calculated as the position of the first peak in the transmitted  $y$ -integrated pulse profile.

bordered by parabolas). A wave-packet with spectrum along one of such curves represents a LW with well defined velocity [22], while quasi-stationary superpositions of LW [9] with defined mean velocity result from spectra well concentrated in the different regions of Fig. 1. In the nonlinear regime, as we show below, the nonlinearity acts as the triggering mechanism of the spectral reshaping of the input into such type of LW. We point out that, though LW exist above the UB edge where they correspond to  $O$ -waves [7], for excitation in the band-gap (regardless whether in proximity of the LB or UB) those playing a role are those below the LB edge, which are of the X type [7] due to the opposite curvatures.

*Numerical method.* — We consider the boundary value problem given by Eqs. (1) subject to unidirectional (forward) gaussian excitation

$$u_+(t, x, z = -L) = u_0 \exp \left[ -\frac{(t - t_s)^2}{t_0^2} - \frac{y^2}{y_0^2} \right] \exp(-i\bar{\omega}t) \quad (2)$$

and  $u_-(t, y, z = L) = 0$ , where  $\bar{\omega}$  is the frequency (energy) detuning that fixes the position in the gap, and  $E = \pi u_0^2 t_0^2 y_0^2$  is the input square norm (fluence). Though we have performed extensive numerical runs, we show below a typical case obtained for  $2L = 4$ ,  $t_s = 30$ ,  $t_0 = 12$ ,  $y_0 = 6$ . Since Eqs. (1) and (2) cannot be solved by standard beam-propagation techniques [20] (the main difficulty arises from the presence of a finite integration region in the propagation direction  $z$  and an infinite transverse domain in  $y$ ), we adopted a pseudo-spectral technique based on a Chebishev-collocation approach along  $z$ , in conjunction with second-order split-step (evolution variable  $t$ , Fast-Fourier transform in  $y$ ) [21].

*Lower branch excitation.* — In Fig. 2a we show the transmission  $\mathcal{T}$  for an excitation inside the gap in proximity of the LB. At low fluence  $E$  there is a residual transmission (owing to the finite size of the system), which decreases at moderate fluences consistently with the nonlinear shift of the gap toward lower frequencies (energies). However, at sufficiently high fluences, the transmission increases with  $E$ . This nonlinear self-transparency cannot be ascribed to stable GB, which do not exist close to the LB [13] (on the LB gap soliton are unstable even in the plane wave limit  $\nabla_y^2 = 0$ ). However, the phenomenon can

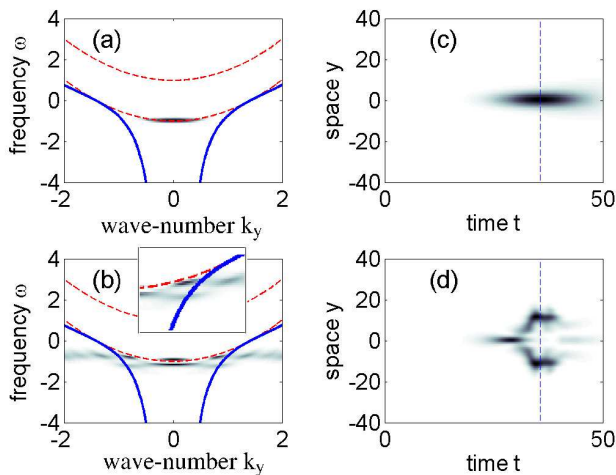


FIG. 3: (Color online) (a,b) Output spectrum of  $u_+$  at (a) low fluence  $E = 1$ , (b) high fluence  $E = 120$  (inset: zoom around  $k_y \cong 1$ ). The red dashed line denotes the forbidden band, the blue thick line is the LW light-line. (c,d) corresponding output spatio-temporal profile for (c)  $E = 1$ ; (d)  $E = 120$ . The vertical dashed line gives the reference instant of the peak of  $|u_+|^2$  at  $E = 1$ .

be explained by looking at the spectra and  $t-y$  snapshots (top view) of the fields at the output ( $z = L$ ). In Fig. 3 we compare the case of low ( $E = 1$ ) and high ( $E = 120$ ) fluence. While the output  $k_y - \omega$  spectrum at  $E = 1$  is well concentrated in the gap around small wave-numbers (Fig. 3a), at high fluence the strong self-focusing causes the spatial spectrum to widen and fill the region of large wave-numbers (Fig. 3b). As also evident in the inset, the energy is progressively concentrated in proximity of the LW light-line, with a clear peak in the region of fast LW, arising from tunneling in wave-number outside the band-gap. Correspondingly the  $t-y$  snapshots show an almost undistorted (nearly gaussian) beam at low fluences (Fig. 3c), which at large fluences, develops clear conical tails along the trailing edge (Fig. 3d). Importantly the leading edge of the pulse arrives earlier in the nonlinear case consistently with the spectral peak in the region of fast LW. However, also spectral components in the region of slow LW are present as clear from the inset in Fig. 3b. The interplay between these two components explains the behavior of the output delay vs.  $E$  displayed in Fig. 2b. As  $E > 50$ , the enhanced transparency of the structure is accompanied by a growing (with  $E$ ) delay. This corresponds to the excitation of slow LW components (see Fig. 3b). However we also found that energy is coupled to frequencies in the region between the lower band-edge and the LW light-line (see inset in Fig. 3b). The latter process becomes dominant at large  $E$ , being responsible for the delay to decrease with  $E$ , for  $E > 100$ . In the spatio-temporal domain, the fast LW corresponds to a bell-shaped leading edge of the transmitted pulse, while the slow LW can be associated to slow conical tails, as

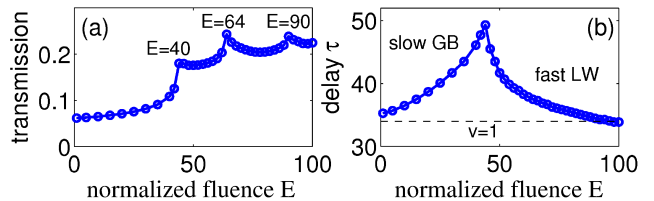


FIG. 4: (Color online) As in Fig. 2 for  $\bar{\omega} = 0.99$  (LB).

shown in Fig. 3d.

*Upper branch excitation.* — The excitation in the proximity of the UB is characterized by the existence of GB which provide the main tunnelling mechanism [13]. Evidence of this process is reported in Fig. 4a, showing that the transmission  $\mathcal{T}$  increases abruptly around  $E \simeq 40$ . Above this threshold,  $\mathcal{T}$  remains high, while it exhibits clear peaks. In addition, as shown in Fig. 4b, the delay versus fluence  $E$  displays a cusp in correspondence with the threshold. This implies that the generated nonlinear waves have a decreasing velocity for increasing fluence up to the threshold value, after which this trend is reversed.

This dynamics is a direct consequence of the multi-dimensional nature of the problem and the existence of LW solutions. In Fig. 5a,d we show the  $k_y - \omega$  spectrum and  $(y, t)$  snapshot at the output  $z = L$ , in correspondence of the first peak in the transmission  $\mathcal{T}$ . As shown, the tunneling wave-packet has a spectrum which remains well confined inside the gap around low wave-numbers. Correspondingly the beam, which has undergone self-focusing in the transverse variable, has substantially bell-shaped section (elliptical top view) with very weak V-shaped tails. Such evolution indicates that the transmission peak is basically associated with the formation of a GB tunneling through the lattice. The situation remains nearly unchanged until the second peak of transmission at  $E = 64$  is reached. Here, the situation is radically different as clear from the spectrum in Fig. 5b. Owing to strong self-focusing, a component of the spectrum has clearly tunneled (mainly horizontally, i.e. in  $k_y$ ) through the gap to the LB. In  $t, y$  domain this spectral feature has one to one correspondence (as can be shown by filtering and anti-transformation) with the strong enhancement of the V-shaped tails characteristic of X waves (see Fig. 5e). Since the LB spectral component lies in the region of fast LW (i.e., the tiny region between the LW light-line and the band-edge), we conclude that the transmission peak is associated with the concomitant excitation of a such type of waves. The fast character of the LW of the X type is also clear from Fig. 5e, which shows that the tails emanate from a wave component that anticipates the slow GB component. The tunnelling process due to the generation of the fast X-wave goes on until the fluence is increased up to the next transmission peak at  $E = 90$  (see Fig. 4a), where a sec-

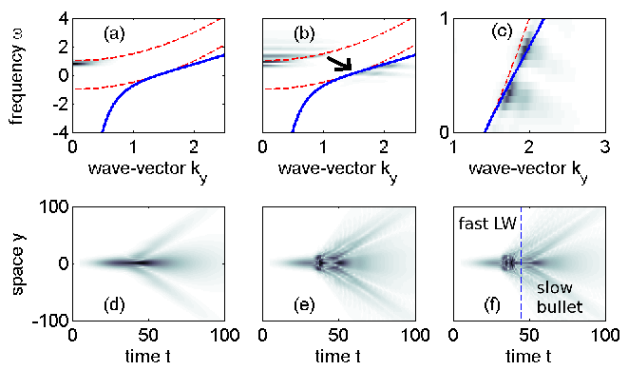


FIG. 5: (Color online) Output features of  $u_+$  for UB excitation ( $\bar{\omega} = 0.99$ ). Output spectra (a)  $E = 40$ , (b)  $E = 64$ , (c)  $E = 90$  (zoom around LW light-line); Corresponding intensity ( $t, y$ ) profiles: (d)  $E = 40$ , (e)  $E = 64$ , (f)  $E = 90$ . The dashed line in (e,f,g) gives the reference instant corresponding to peak of  $|u_+|^2$  at  $E = 40$ .

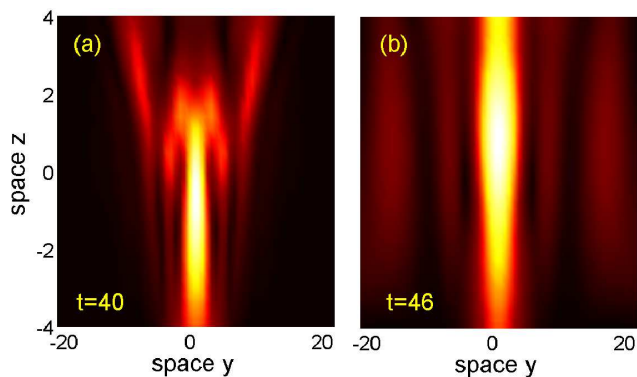


FIG. 6: (Color online) Level plot of spatial intensity  $|u_+|^2 + |u_-|^2$  for UB excitation ( $\bar{\omega} = 0.99$ ), at two instants: (a)  $t = 40$ , both the fast conical LW and the GB are trapped in the lattice; (b)  $t = 46$ , the fast LW has left the lattice and only the slow GB remains.

ond LW is generated, as shown by the splitting of the LB spectral component (see Fig. 5c), and the more structured fast wave component in Fig. 5f. The excitation of a fast LW explains the cusp in the delay time  $\tau$  in Fig. 4b: as energy is increased the bullet develops fast LW tails that eventually precede the GB and correspondingly (cusp in Fig. 4b) the delay starts to decrease with  $E$ . This process is even more evident in Fig. 6, where we show the intensity profile for  $E = 50$  and  $2L = 8$  (a longer structure makes the process more evident), at two different instants. For  $t = 40$ , the intensity distribution clearly unveils a X-shaped pulse which is in proximity of the output. At  $t = 46$  the fast LW has left the structure, and only the slow GB remains.

*Conclusions.* — In summary the study of transverse effects a 1D Bragg lattice unveils the role of fast and slow LW, characterized by specific spatio-temporal spectra. Their excitation foster a variety of self-transparency

effects, either in conjunction with multi-dimensional gap solitons, or as an alternative to them. Measuring the spatio-temporal spectra or the trend of the output delay with input fluence could be used to monitor the excitation of LW. Our results have implication in all of the field where multi-dimensional solitary wave and periodicity play a role, and more specifically in Bose Einstein condensation and nonlinear optics.

We thank INFM-CINECA initiative for parallel computing and MIUR for financial support. A.D.F. is supported by the Consortium of Speckled Computing (EP-SRC “Specknet”).

\* Electronic address: claudio.conti@phys.uniroma1.it

- [1] P. Di Trapani *et al.*, Phys. Rev. Lett. **91**, 093904 (2003).
- [2] C. Conti *et al.*, Phys. Rev. Lett. **90**, 170406 (2003); C. Conti, Phys. Rev. E **70**, 046613 (2004).
- [3] M. Kolesik, E.M. Wright, and J. V. Moloney, Phys. Rev. Lett. **92**, 253901 (2004).
- [4] D. Faccio, M. Porras, A. Dubietis, F. Bragheri, A. Couairon, P. Di Trapani, Phys. Rev. Lett. **96**, 193901 (2006).
- [5] Y. Lahini, E. Frumker, Y. Silberberg, S. Droulias, K. Hizanidis, and D. N. Christodoulides, Phys. Rev. Lett. **98**, 023901 (2007); S. Droulias, K. Hizanidis, J. Meier, and D. N. Christodoulides, Opt. Exp. **13**, 1827 (2005).
- [6] J. Lu and J. F. Greenleaf, IEEE Trans. Ultrason. Ferr. elec. Freq. contr. **39**, 441 (1992); P. Saari and K. Reivelt, Phys. Rev. Lett. **79**, 4135 (1997).
- [7] M. Porras and P. Di Trapani Phys. Rev. E **69**, 066606 (2004).
- [8] E. Recami, M. Zamboni-Rached, and H.E. Hernandez-Figueroa, *Localized waves* (Wiley, 2007).
- [9] C. Conti, S. Trillo, Phys. Rev. Lett. **92**, 120404 (2004).
- [10] S. Longhi and D. Janner, Phys. Rev. B **70**, 235123 (2004); S. Longhi, Phys. Rev. E **71**, 016603 (2005).
- [11] K. Staliunas and R. Herrero, Phys. Rev. E **73**, 016601 (2006).
- [12] S. John and N. Aközbek, Phys. Rev. Lett. **71**, 1168 (1993); A. Aceves, B. Costantini, C. De Angelis, J. Opt. Soc. Am. B **12**, 1475 (1995); N. Aközbek, and S. John, Phys. Rev. E **57**, 2287 (1998); A. B. Aceves, G. Fibich, B. Ilan, Physica D **189**, 277 (2004).
- [13] T. Dohnal, A. B. Aceves, Stud. Appl. Math. **115**, 209 (2005).
- [14] A. Sukhorukov and Y. S. Kivshar, Phys. Rev. Lett. **97**, 233901 (2006).
- [15] W. Chen and D. L. Mills, Phys. Rev. Lett. **58**, 160 (1987); C. M. de Sterke and J. E. Sipe, Phys. Rev. A **39**, 5163 (1988); A. B. Aceves and S. Wabnitz, Phys. Lett. A **141**, 37 (1989); D. N. Christodoulides and R. I. Joseph, Phys. Rev. Lett. **62**, 1746 (1989).
- [16] B. J. Eggleton, R. E. Slusher, C. M. de Sterke, P. A. Krug, and J. E. Sipe, Phys. Rev. Lett. **76**, 1627 (1996).
- [17] J. T. Mok, C. M. De Sterke, I. C. M. Littler, and B. J. Eggleton, Nature Phys. **2**, 775 (2006).
- [18] D. Mandelik, R. Morandotti, J.S. Aitchison, and Y. Silberberg, Phys. Rev. Lett. **92**, 093904 (2004). D. Neshev, A. Sukhorukov, B. Hanna, W. Krowlikowsky, and Y. S. Kivshar, Phys. Rev. Lett. **93**, 083905 (2004).

- [19] S. Pötting, P. Meystre, and E. M. Wright, in *Nonlinear photonic crystals* (Springer, 2003), vol. 10 of *Photonics*; B. Eiermann *et al.*, Phys. Rev. Lett. **92**, 230401 (2004). O. Morsch and M. K. Oberthaler, Rev. Mod. Phys. **78**, 179 (2006).
- [20] G. P. Agrawal, *Nonlinear fiber optics* 3rd ed. (Academic Press, San Diego, 2001)
- [21] J. P. Boyd, *Chebyshev and Fourier Spectral Methods* II ed. (Dover, New York, 2001); C. Canuto, M. Y. Hussaini, A. Quatroni and T. A. Zhang, *Spectral Methods for Fluid Dynamics* (Springer-Verlag, New York, 1988)
- [22] The LW ( $\psi_+$ ,  $\psi_-$ ) can be expressed as integral superposition of Bessel functions, as we will show elsewhere. There is no explicit expression for such integrals.